Advances in Materials Research, *Vol. 11*, *No. 2* (*2022*) *91-109*
https://doi.org/10.12989/amr.2022.11.2.091

Rehabilitation of RC structural elements: Application for continuous beams bonded by composite plate under a prestressing force

Rabahi Abderezak, Benferhat Rabia and Tahar Hassaine Daouadji*

Department of Civil Engineering, *Laboratory of Geomatics and Sustainable Development*, *University of Tiaret*, *Algeria*

(*Received July 7*, *2021*, *Revised November 2*, *2021*, *Accepted November 10*, *2021*)

Abstract. This paper presents a closed-form higher-order analysis of interfacial shear stresses in RC continuous beams strengthened with bonded prestressed laminates. For retrofitting reinforced concrete continuous beams is to bond fiber reinforced prestressed composite plates to their tensile faces. An important failure mode of such plated beams is the debonding of the composite plates from the concrete due to high level of stress concentration in the adhesive at the ends of the composite plate. The model is based on equilibrium and deformations compatibility requirements in and all parts of the strengthened beam, where both the shear and normal stresses are assumed to be invariant across the adhesive layer thickness. In the present theoretical analysis, the adherend shear deformations are taken into account by assuming a parabolic shear stress through the thickness of both the RC continuous beams strengthened with bonded prestressed laminates. The theoretical predictions are compared with other existing solutions. A parametric study has been conducted to investigate the sensitivity of interface behavior to parameters such as laminate stiffness and the thickness of the laminate where all were found to have a marked effect on the magnitude of maximum shear and normal stress in the composite member.

Keywords: composite plate; continuous RC beam; interfacial stresses; shear lag effect; strengthening

1. Introduction

In recent years, the external bonding of composite plates the beam tension face has become a common practice and is widely used to strengthen or repair structures. Strengthening RC beams in flexure with FRP plates is a powerful strengthening technique due to its simplicity of in situ application, small increase of the beam size and weight, and good resistance to corrosion. Extensive research efforts have been carried out to study and model the behavior of simply supported beams with external FRP plates; as a result, there are many design guidelines for such beams (Smith and Teng 2002, Daouadji *et al*. 2021a, Benferhat *et al*. 2021b, Tounsi 2006, Abderezak *et al*. 2021d, and Daouadji 2017). However, many in situ RC beams are used in continuous construction; there has been very limited research into the behavior of such beams with external strengthening. Many studies show that the use of composite plates to strengthen continuous beams was effective for reducing deflections and for increasing their load carrying

*Corresponding author, Ph.D., Professor, E-mail: daouadjitahar@gmail.com; tahar.daouadji@univ-tiaret.dz

http://www.techno-press.org/?journal=amr&subpage=5 ISSN: 2234-0912 (Print), 2234-179X (Online)

capacity (Benferhat *et al*. 2021a, Rabahi *et al*. 2021a, Daouadji *et al*. 2021c, Tayeb *et al*. 2021, Tlidji *et al*. 2021b and Hadj *et al*. 2021).

Analysis of interfacial stress in beams with bonded plates has been performed by several researchers (Antar *et al*. 2019, Zohra *et al*. 2021, Abderezak *et al*. 2021f, Civalek and Avcar 2020b, Gomes *et al*. 2021, Wang *et al*. 2020a, Tanzadeh and Amoushahi 2020, Hirwani and Panda 2020, Anil *et al*. 2020, Mohammad *et al*. 2020, Chedad *et al*. 2018, Krour *et al*. 2014, Aicha *et al*. 2020, Benferhat *et al*. 2020a, Benferhat *et al*. 2020b, Abderezak *et al*. 2020, Daouadji *et al*. 2020, Panjehpour *et al*. 2014, Wang *et al*. 2021, Cheng *et al*. 2020, Zeverdejani and Beni 2020, Henni *et al*. 2021, Bensatallah *et al*. 2020, Abderezak *et al*. 2021e, Tlidji *et al*. 2021a and Yuan *et al*. 2019). The analyses provided closed-form formulas for the calculation of interfacial shear and peeling stress in beams with bonded non-prestressed plates or laminates. However, the problem of interfacial stress when prestressed laminates are used in strengthening and repair has treated by Daouadji *et al*. (2021e), Abderezak *et al*. (2019) and Benachour *et al*. (2008). In this investigation, only interfacial shear stress was studied and the analyzed beam was not loaded (Guenaneche and Tounsi 2014, Benferhat *et al*. 2021c, Henriques *et al*. 2020, Daouadji *et al*. 2019, 2021b, Liu *et al*. 2019, Panjehpour *et al*. 2016, Abderezak *et al*. 2021b, c, Larrinaga *et al*. 2020, Daraei *et al*. 2020, Chen *et al*. 2020, Civalek and Avcar 2020a, Mercan *et al*. 2020, Kalita *et al*. 2020, Keshav and Patel 2020, Tounsi *et al*. 2008, He *et al*. 2019).

In this paper, a general new solution is developed to predict both shear and normal interfacial stress in continuous RC beam strengthened with bonded prestressed composite plate. The considered beam is subjected to a uniformly distributed load, compared with the existing solutions such as presented by Daouadji *et al*. (2021d), Benachour (2008) and Rabahi *et al*. (2016), the present model is general in nature, and it is applicable to more general loads cases. With the escalating use of this strengthening scheme, there is a great need for calculation models that can be used to predict the magnitude of maximum interfacial stress at the end of the laminate. There is also some lack of knowledge today regarding how material and geometric properties of the strengthening system should be chosen in order to minimize the magnitude of these interfacial stresses and ensure sufficient strength of the strengthening system without need for expensive and complicated mechanical anchorage devices.

2. Method of solution

2.1 Basic assumptions

To simplify the theoretical derivations of interfacial stresses in Continuous RC beam bonded by a prestressed composite plate (Fig. 1), the following assumptions are adopted in this article. Figs. 1 and 2 shows the geometric model for structure and shows a schematic sketch of the steps involved in strengthening a beam with a bonded prestressed laminate. Po (Po_1, Po_2) is the initial prestressing force in the laminate, Figs. 3 and 4 shows an infinitesimal element of prestressed composite-strengthened continuous RC beam, as shown in Fig. 3 “Span area”, and as shown in Fig. 4 “Cantilevered area”. The present analysis takes into consideration the transverse shear stress and strain in the beam and the plate but ignores the transverse normal stress in them. One of the analytical approaches proposed by Abderezak *et al*. (2019) for RC beam strengthened with a bonded prestressed composite plate (Figs. 1 and 2) was used in order to compare it with other analytical solutions.

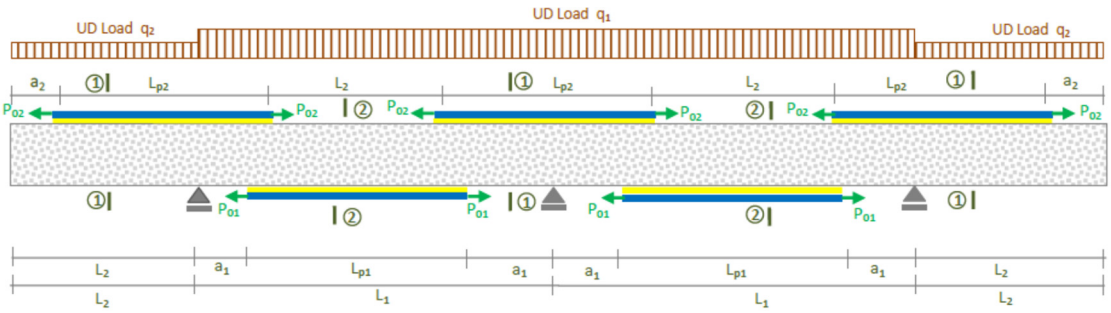

Fig. 1 Continuous RC beam bonded by a prestressed composite plate

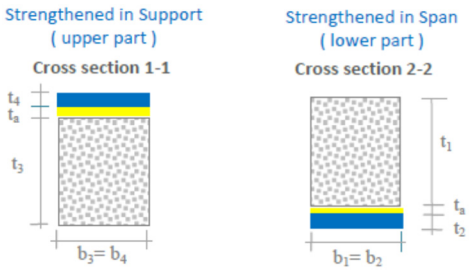

Fig. 2 Continuous RC beam bonded by a prestressed composite plate: cross section in span and on both supports

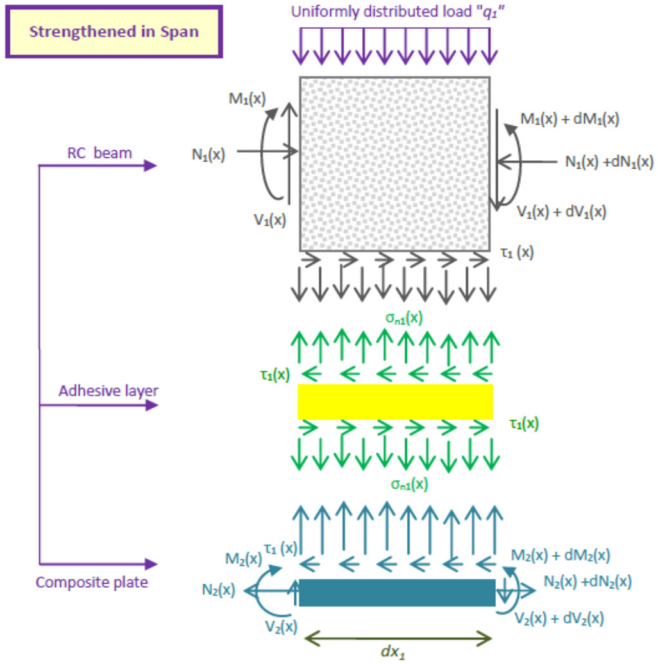

Fig. 3 Forces in infinitesimal element of a continuous RC beam bonded by a prestressed composite plate: Span area

The analytical approach is based on the following assumptions (Abderezak *et al*. 2019):

(1) Elastic stress strain relationship for RC beam, prestressed composite plate and adhesive;
(2) There is a perfect bond between the prestressed composite plate and the RC beam;
(3) The adhesive is assumed to only play a role in transferring the stresses from the RC beam to the prestressed composite plate reinforcement;
(4) The stresses in the adhesive layer do not change through the direction of the thickness;

2.2 Mathematical formulation of the present method "*Strengthened in Span*"

A differential section *dx*, can be cutout from the composite- strengthened continuous RC beam, as shown in Fig. 3 "*Strengthened in Span*". The strains in the continuous RC beam near the adhesive interface and the external FRP reinforcement can be expressed in this theory.

2.2.1 Shear stress distribution along the FRP–RC beam interface "*Strengthened in Span*"

The following governing differential equation for the interfacial normal stress (Abderezak *et al*. 2019)

$$\frac{d^2\tau(x)}{dx^2} - \frac{b_2\left[\frac{(y_1+y_2)(y_1+y_2+t_a)}{E_1I_1+E_2I_2}+\frac{1}{E_1A_1}+\frac{1}{E_2A_2}\right]}{\frac{t_a}{G_a}+\frac{t_1}{4G_1}+\frac{5t_2}{12G_2}}\tau(x) + \frac{\left[\frac{y_1+y_2}{E_1I_1+E_2I_2}\right]}{\frac{t_a}{G_a}+\frac{t_1}{4G_1}+\frac{5t_2}{12G_2}}V_{T_{1-2}}(x) = 0 \tag{1}$$

For simplicity, the general solutions presented below are limited to loading which is either concentrated or uniformly distributed over part or the whole span of the beam, or both. For such loading, $d^2V_T(x)/dx^2 = 0$, and the general solution to Eq. (1) is given by

$$\tau(x) = \eta_1\, cosh(\xi x) + \eta_2\, sinh(\xi x) + \frac{(t_1+t_2)}{2\xi^2\left(\frac{t_a}{G_a}+\frac{t_1}{4G_1}+\frac{5t_2}{12G_2}\right)(E_1I_1+E_2I_2)}V_{T1-2}(x) \tag{2}$$

Where

$$\xi = \sqrt{\frac{b_2\left[\frac{(t_1+t_2)(t_1+t_2+2t_a)}{4(E_1I_1+E_2I_2)}+\frac{1}{E_1A_1}+\frac{1}{E_2A_2}\right]}{\frac{t_a}{G_a}+\frac{t_1}{4G_1}+\frac{5t_2}{12G_2}}} \tag{3}$$

And η_1 and η_2 are constant coefficients determined from the boundary conditions. In the present study, a simply supported beam has been investigated which is subjected to a uniformly distributed load. For our case of a uniformly distributed load, the formula of the shear stress is given by the following equation

$$\tau(x) = \left[\frac{1}{\xi}\left(\frac{t_a}{G_a} + \frac{t_1}{4G_1} + \frac{5t_2}{12G_2}\right)\left(\frac{A_{11}^{`}}{b_2}\right)P_{0_1} - \frac{y_1 M_{t_{1-2}}(0)}{E_{\ 1}I_1}\right]e^{-\xi x} + \frac{(t_1+t_2)\left(a_1 q_1 + x - \frac{e^{-\xi x}}{\xi}q_1\right)}{2\xi^2\left(\frac{t_a}{G_a} + \frac{t_1}{4G_1} + \frac{5t_2}{12G_2}\right)(E_1I_1 + E_2I_2)} \quad (4)$$
$$0 \le x \le L_{P_1}$$

2.2.2 Normal stress distribution along the FRP—RC beam interface "*Strengthened in Span*"

The following governing differential equation for the interfacial normal stress (Abderezak *et al*. 2019)

$$\frac{d^4\sigma_n(x)}{dx^4} + \frac{E_a b_2}{t_a}\left(\frac{1}{E_1I_1} + \frac{1}{E_2I_2}\right)\sigma_n(x) + \frac{E_a b_2}{t_a}\left(\frac{y_1}{E_1I_1} - \frac{y_2}{E_2I_2}\right)\frac{d\tau(x)}{dx} + \frac{qE_a}{t_aE_1I_1} = 0 \quad (5)$$

The general solution to this fourth–order differential equation is

$$\sigma_n(x) = e^{-\alpha x}[\eta_3\, cos(\alpha x) + \eta_3\, sin(\alpha x)] + e^{\alpha x}[\eta_5\, cos(\alpha x) + \eta_6\, sin(\alpha x)] - \left[\frac{y_1E_2I_2 - y_2E_1I_1}{E_1I_1 + E_2I_2}\right]\frac{d\tau(x)}{dx} - \left[\frac{E_2I_2}{b_2(E_1I_1 + E_2I_2)}\right]q_1 \quad (6)$$

For large values of x it is assumed that the normal stress approaches zero and, as a result, $\eta_5 = \eta_6 = 0$. The general solution therefore becomes

$$\sigma_n(x) = e^{-\alpha x}[\eta_3\, cos(\alpha x) + \eta_4\, sin(\alpha x)] - \frac{y_1E_2I_2 - y_2E_1I_1}{E_1I_1 + E_2I_2}\frac{d\tau(x)}{dx} - \frac{E_2I_2}{b_2(E_1I_1 + E_2I_2)}q_1 \quad (7)$$

Where

$$\alpha = \sqrt[4]{\frac{E_a b_2}{4t_a}\left(\frac{1}{E_1I_1} + \frac{1}{E_2I_2}\right)} \quad (8)$$

As is described by Tounsi (2006), the constants η_3 and η_4 in Eq. (7) are determined using the appropriate boundary conditions and they are written as follows

$$\eta_3 = \frac{E_a[V_{T1-2}(0) + \alpha M_{T1-2}(0)]}{2\alpha^2E_1I_1} - \frac{E_a}{t_a 2\alpha^3}\left(\frac{y_1b_2}{E_1I_1} - \frac{y_2b_2}{E_2I_2}\right)\tau(0) + \frac{y_1E_2I_2 - y_2E_1I_1}{2\alpha^3(E_1I_1 + E_2I_2)}\left(\frac{d^4\tau(0)}{dx^4} + \alpha\frac{d^3\tau(0)}{dx^3}\right) \quad (9)$$

$$\eta_4 = \frac{-E_aM_{T1-2}(0)}{2\alpha^2t_aE_1I_1} - \frac{y_1E_2I_2 - y_2E_1I_1}{2\alpha^2(E_1I_1 + E_2I_2)}\frac{d^3\tau(0)}{dx^3} \quad (10)$$

The above expressions for the constants η_3 and η_4 have been left in terms of the bending

moment $M_{T1\text{-}2}(0)$ and shear force $V_{T1\text{-}2}(0)$ at the end of the soffit plate. With the constants η_3 and η_4 determined, the interfacial normal stress can then be found using Eq. (7).

2.3 Mathematical formulation of the present method "Strengthened in Support"

A differential section dx, can be cutout from the composite- strengthened continuous RC beam, as shown in Fig. 4 "*Strengthened in Support*". The strains in the continuous RC beam near the adhesive interface and the external FRP reinforcement can be expressed in this theory.

2.3.1 Shear stress distribution along the FRP- RC beam interface "Strengthened in Support"

The following governing differential equation for the interfacial normal stress (Abderezak *et al.* 2019)

$$\frac{d^2\tau(x)}{dx^2} - \frac{G_a}{t_a}\left[A'_{11} + \frac{b_4}{E_3A_3} + \frac{\left(y_3+\frac{t_4}{2}\right)\left(y_3+t_a+\frac{t_4}{2}\right)}{E_3I_3D'_{11}+b_4}b_4D'_{11}\right]\tau(x) + \frac{G_a}{t_a}\left[\frac{\left(y_3+\frac{t_4}{2}\right)}{E_3I_3D'_{11}+b_4}\right]V_{T3-4}(x) = 0 \tag{11}$$

The solution to the differential equation (Eq. (11)) above is given by

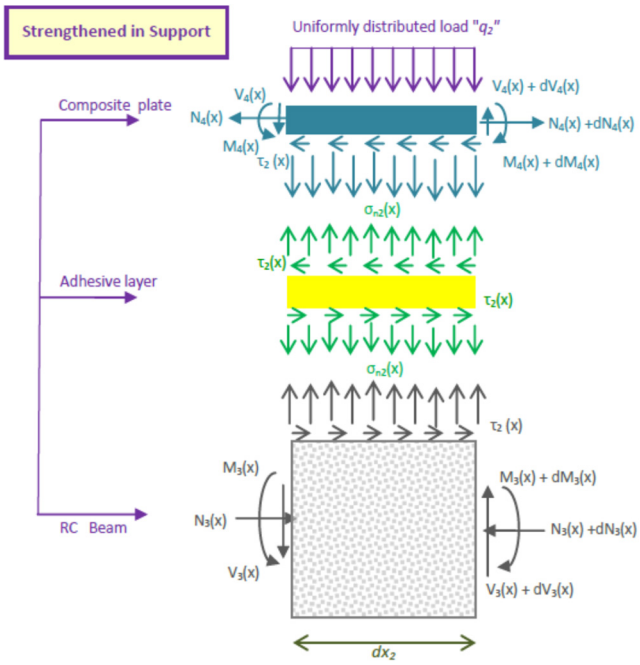

Fig. 4 Forces in infinitesimal element of a continuous RC beam bonded by a prestressed composite plate: Cantilevered area

$$\tau(x) = \eta_7\, cosh(\delta x) + \eta_8\, sinh(\delta x) + \left[\frac{1}{2\delta^2}\left(\frac{t_a}{G_a} + \frac{t_3}{4G_3} + \frac{5t_4}{12G_4}\right)\left(\frac{(2y_3 + t_4)}{E_3 I_3 D_{11}^{'} + b_4} D_{11}^{'}\right)\right] V_{T3-4}(x) \tag{12}$$

With

$$\delta = \left[\frac{A_{11}^{'} + \frac{b_4}{E_3 A_3} + \frac{(2y_3 + t_4)(2y_3 + 2t_a + t_4)}{4E_3 I_3 D_{11}^{'} + b_4} b_4 D_{11}^{'}}{\frac{t_a}{G_a} + \frac{t_3}{4G_3} + \frac{5t_4}{12G_4}}\right]^{\frac{1}{2}} \tag{13}$$

For our case of a uniformly distributed load, the formula of the shear stress is given by the following equation

$$\tau(x) = \eta_8 e^{-\delta x} + \left[\frac{1}{2\delta^2}\left(\frac{t_a}{G_a} + \frac{t_3}{4G_3} + \frac{5t_4}{12G_4}\right)\left(\frac{(2y_3 + t_4)}{E_3 I_3 D_{11}^{'} + b_4}\right) D_{11}^{'}\right] q_2(a_2 + x) \tag{14}$$

$$0 \le x \le L_{P2}$$

With

$$\eta_8 = \frac{1}{\delta}\left(\frac{t_a}{G_a} + \frac{t_3}{4G_3} + \frac{5t_4}{12G_4}\right)\left(\frac{A_{11}^{'}}{b_4} P_{02} - \frac{y_1 M_{t_{3-4}}(0)}{E_{\ 3} I_3}\right) - \left[\frac{1}{2\delta^2}\left(\frac{t_a}{G_a} + \frac{t_3}{4G_3} + \frac{5t_4}{12G_4}\right)\left(\frac{(2y_3 + t_4)}{E_3 I_3 D_{11}^{'} + b_4}\right) D_{11}^{'}\right]\frac{q_2}{\delta} \tag{15}$$

2.3.2 Normal stress distribution along the FRP- RC beam interface "Strengthened in Support"

The following governing differential equation for the interfacial normal stress (Abderezak *et al*. 2019)

$$\frac{d^4\sigma_n(x)}{dx^4} + \frac{E_a}{t_a}(D_{11}^{'} + \frac{b_4}{E_3 I_3})\sigma_n(x) - \frac{E_a}{t_a}(D_{11}^{'}\frac{t_4}{2} - \frac{y_3 b_4}{E_3 I_3})\frac{d\tau(x)}{dx} + \frac{q_2 E_a}{E_3 I_3 t_a} = 0 \tag{16}$$

The general solution to this fourth–order differential equation is

$$\sigma_n(x) = e^{-\Delta x}[\eta_9\, cos(\Delta x) + \eta_{10}\, sin(\Delta x)] + e^{\Delta x}[\eta_{11}\, cos(\Delta x) + \eta_{12}\, sin(\Delta x)] - \frac{2y_3 b_4 - D_{11}^{'} E_3 I_3 t_4}{2D_{11}^{'} E_3 I_3 + b_4}\frac{d\tau(x)}{dx} - \frac{q_2}{D_{11}^{'} E_3 I_3 + b_4} \tag{17}$$

For large values of x it is assumed that the normal stress approaches zero and, as a result, $\eta_{11} = \eta_{12} = 0$. The general solution therefore becomes

$$\sigma_n(x) = e^{-\Delta x}[\eta_9\, cos(\Delta x) + \eta_{10}\, sin(\Delta x)] - \frac{2y_3 b_4 - D_{11}^{'} E_3 I_3 t_4}{2D_{11}^{'} E_3 I_3 + b_4}\frac{d\tau(x)}{dx} - \frac{q_2}{D_{11}^{'} E_3 I_3 + b_4} \tag{18}$$

Where

$$\Delta = \left[\frac{E_a}{4t_a}\left(D_{11}^{'} + \frac{b_4}{E_3 I_3}\right)\right]^{\frac{1}{4}} \tag{19}$$

As is described by Daouadji *et al*. (2019), the constants η_9 and η_{10} in Eq. (18) are determined using the appropriate boundary conditions and they are written as follows

$$\begin{aligned}\eta_9 = {} & \frac{\frac{E_a}{E_3 I_3 t_a}}{2\left[\frac{E_a}{4t_a}\left(D_{11}^{'} + \frac{b_4}{E_3 I_3}\right)\right]^{\frac{3}{4}}}\left[V_{T3-4}(0) + \Delta M_{T3-4}(0)\right] - \frac{\frac{b_4 E_a}{t_a}\left[\frac{y_3}{E_3 I_3} - \frac{D_{11}^{'} t_4}{2b_4}\right]}{2\left[\frac{E_a}{4t_a}\left(D_{11}^{'} + \frac{b_4}{E_3 I_3}\right)\right]^{\frac{3}{4}}}\tau(0) \\ & + \frac{\frac{2y_3 b_4 - D_{11}^{'} E_3 I_3 t_4}{2D_{11}^{'} E_3 I_3 + b_4}}{2\left[\frac{E_a}{4t_a}\left(D_{11}^{'} + \frac{b_4}{E_3 I_3}\right)\right]^{\frac{3}{4}}}\left(\frac{d^4\tau(0)}{dx^4} + \left[\frac{E_a}{4t_a}\left(D_{11}^{'} + \frac{b_4}{E_3 I_3}\right)\right]^{\frac{1}{4}}\frac{d^3\tau(0)}{dx^3}\right)\end{aligned} \tag{20}$$

$$\begin{aligned}\eta_{10} = {} & -\frac{E_a}{2\left[\frac{E_a}{4t_a}\left(D_{11}^{'} + \frac{b_4}{E_3 I_3}\right)\right]^{\frac{1}{2}} E_3 I_3 t_a} M_{T3-4}(0) \\ & - \frac{2y_3 b_4 - D_{11}^{'} E_3 I_3 t_4}{2(2D_{11}^{'} E_3 I_3 + b_4)\left[\frac{E_a}{4t_a}\left(D_{11}^{'} + \frac{b_4}{E_3 I_3}\right)\right]^{\frac{1}{2}}}\frac{d^3\tau(0)}{dx^3}\end{aligned} \tag{21}$$

The above expressions for the constants η_9 and η_{10} has been left in terms of the bending moment $M_T(0)$ and shear force $V_T(0)$ at the end of the soffit plate. With the constants η_9 and η_{10} determined, the interfacial normal stress can then be found using Eq. (18).

3. Numerical results and discussions

3.1 Geometric and material properties

The material used for the present studies is a continuous RC beam bonded by a prestressed composite plate. The steel continuous beam is subjected to a uniformly distributed load.

A summary of the geometric and material properties is given in Table 1 and Fig. 5. The span of the steel continuous beam is (L_{p1} = 2600 mm, L_{p2} = 1500 mm), the distance from the support to the end of the plate is a_1 = 200 mm and a_2 = 500 mm, the uniformly distributed load is q_1 = 50 kN/ml and q_2 = 30 kN/ml and the single point distributed load Q_1 = 150 kN and Q_2 = 50 kN.

3.2 Comparison of analytical solution

Comparison with other solutions: To verify the analytical model, the present predictions are compared firstly with those of Abderezak *et al*. (2019) and He *et al*. (2019) in the case of the absence of the prestressing force and in the second time the present method is compared with that developed by Abderezak *et al*. (2019) in the case where only the prestressing force is applied.

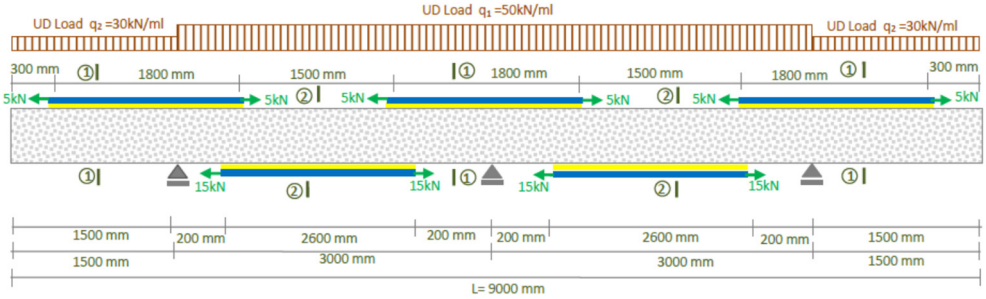

(a) Case of uniformly distributed loads

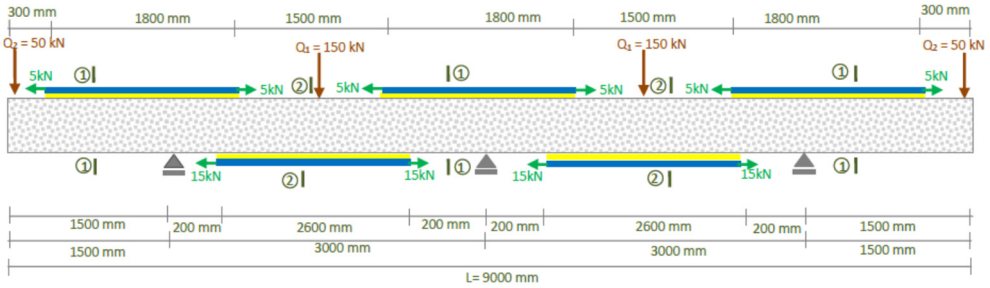

(b) Case of concentrated loads

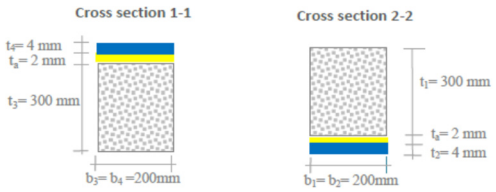

(c) Cross sections

Fig. 5 Geometric characteristic of a continuous RC beam bonded by a prestressed composite plate: (a) case of uniformly distributed loads; (b) case of concentrated loads; and (c) cross sections

Table 1 Geometric and mechanical properties of the materials used

Component	Width (mm)	Depth (mm)	Young's modulus (MPa)
RC beam	$b_1 = b_3 = 100$	$t_1 = 300$	$E_1 = 30000$
Adhesive layer	$b_1 = b_3 = 100$	$t_a = 2$	$E_a = 3000$
Sika Carbodur	$b_2 = b_4 = 100$	$t_2 = 4$	$E_2 = 165{,}000$
Sika wrap	$b_2 = b_4 = 100$	$t_2 = 0{,}48$	$E_2 = 230{,}000$
Carbone HR	$b_2 = b_4 = 100$	$t_2 = 4$	$E_2 = 140{,}000$
Glass E	$b_2 = b_4 = 100$	$t_2 = 4$	$E_2 = 73{,}000$

Adhesive stresses without prestressing force ($P_{01} = 0$ and $P_{02} = 0$): A comparison of the edge interfacial shear and normal stress from the different closed-form solutions reviewed earlier is undertaken in this section (Tables 2 and 3). Two example problems are considered. In the problem, the beam is simply supported and subjected to uniformly distributed load (q_1 = 50 kN/ml

Table 2 Comparison with analytical approach of interfacial shear and normal stresses: ***Strengthened in Span***

Continuous RC Beam bonded with a prestressed thin plate subjected to a uniformly distributed load - *Strengthened in Span* -					
Model	Prestressing load	Strengthened with Sika carbodur plate		Strengthened with four layers of Sika Wrap	
		$\tau(x)$	$\sigma(x)$	$\tau(x)$	$\sigma(x)$
Rabahi Model 2019	P = 0	1.997453	1.18521	1.75330	1.552541
	P = 10 kN	1.489854	0.84512	0.98921	0.907338
Present Analytical Model	P = 0	2.15082	1.23218	1.82756	1.589362
	P = 10 kN	1.53651	0.89909	1.06499	0.939559
	P = 25 kN	0.61506	0.39946	-0.07887	-0.035083
Continuous RC Beam bonded with a prestressed thin plate subjected to a Single Point Distributed Load - *Strengthened in Span* -					
Model	Prestressing load	Strengthened with Sika carbodur plate		Strengthened with four layers of Sika Wrap	
		$\tau(x)$	$\sigma(x)$	$\tau(x)$	$\sigma(x)$
Rabahi Model 2019	P = 0	2.58835	1.47951	2.01991	1.87624
	P = 10 kN	1.30273	0.79952	0.57736	0.53379
Present Analytical Model	P = 0	2.6425	1.5149	2.1918	1.9094
	P = 10 kN	1.3357	0.80356	0.59563	0.54656
	P = 25 kN	-0.62459	-0.26350	-1.7988	-1.4976

Table 3 Comparison with analytical approach of interfacial shear and normal stresses ***- Strengthened in Support -***

Continuous RC Beam bonded with a prestressed thin plate subjected to a uniformly distributed load - *Strengthened in Support* -					
Model	Prestressing load	Strengthened with Sika carbodur plate		Strengthened with four layers of Sika Wrap	
		$\tau(x)$	$\sigma(x)$	$\tau(x)$	$\sigma(x)$
He Model 2019	P = 0	0.528610	0.376412	0.418634	0.458127
Present Analytical Model	P = 0	0.490784	0.347852	0.403380	0.432600
	P = 2 kN	0.213390	0.161925	0.0645439	0.0770386
	P = 5 kN	-0.202700	-0.116964	-0.443710	-0.453604
Model	Prestressing load	Strengthened with Sika carbodur plate		Strengthened with four layers of Sika Wrap	
		$\tau(x)$	$\sigma(x)$	$\tau(x)$	$\sigma(x)$
He Model 2019	P = 0	1.25658	0.74521	1.07416	0.885267
Present Analytical Model	P = 0	1.22440	0.70158	1.02553	0.892055
	P = 2 kN	0.96304	0.559310	0.70327	0.619480
	P = 5 kN	0.55099	0.345892	0.22739	0.210623

and q_2 = 30 kN/ml) and subjected to a Single Point Distributed Load (Q_1 = 150 kN and Q_2 = 50 kN). The results of the peak interfacial shear and normal stress are given in Tables 2 and 3. From the presented results, it can be seen that the present solution agree closely with the other methods.

3.3 Effect of plate stiffness as a function of the variation of the prestressing force on the adhesion stresses

Tables 4 and 5 gives interfacial normal and shear stresses for the RC beam bonded with a Sika carbodur plate, with four layers of Sika Wrap, with Steel plate, with perfect FGM plate and with honeycomb sandwich plate, respectively, which demonstrates the effect of plate material properties on interfacial stresses. The length of the plate is L_{p1} = 2600 mm and L_{p2} = 1800 mm, and the thickness of the plate and the adhesive layer are both 4 mm. The RC continuous beam strengthening with prestressed laminate and submitted under different types of loading by combining between the parameters of loads (q_1; q_2, Q_1, Q_2 and P_{01} P_{02}). The results show that, as the plate material becomes softer (from different plate of reinforcement; cited in Tables 4 and 5), the interfacial stresses become smaller, as expected. This is because, under the same load, the tensile force developed in the plate is smaller, which leads to reduced interfacial stresses. The position of the peak interfacial shear stress moves closer to the free edge as the plate becomes less stiff.

Table 4 Effect of plate stiffness as a function of the variation of the prestressing force of interfacial shear and normal stresses - Strengthened in Span -

Continuous RC Beam bonded with a prestressed thin plate subjected to a uniformly distributed load - *Strengthened in Span* -										
Present Model	Strengthened with Sika carbodur plate		Strengthened with four layers of Sika Wrap		Strengthened with Steel plate		Strengthened with perfect FGM plate		Strengthened with honeycomb sandwich plate	
	τ(x)	σ(x)	τ(x)	σ(x)	τ(x)	σ(x)	τ(x)	σ(x)	τ(x)	σ(x)
P_1 = 0	2.15082	1.23218	1.8276	1.58932	2.3399	1.2820	1.46474	1.01192	1.16299	1.08391
P_1 = 5 kN	1.84367	1.06564	1.4463	1.26445	2.0682	1.14155	0.96799	0.68374	0.522798	0.555768
P_1 = 15 kN	1.22935	0.73254	0.6837	0.61467	1.5247	0.86064	-0.0255	-0.02735	-0.75759	-0.500522
P_1 = 25 kN	0.61506	0.39946	-0.078	-0.03508	0.9813	0.57973	-1.0190	-0.62904	-2.03768	-1.55682
Continuous RC Beam bonded with a prestressed thin plate subjected to a Single Point Distributed Load - *Strengthened in Span* -										
Present Model	Strengthened with Sika carbodur plate		Strengthened with four layers of Sika Wrap		Strengthened with Steel plate		Strengthened with perfect FGM plate		Strengthened with honeycomb sandwich plate	
	τ(x)	σ(x)	τ(x)	σ(x)	τ(x)	σ(x)	τ(x)	σ(x)	τ(x)	σ(x)
P_1 = 0	2.6425	1.5149	2.1918	1.9094	2.9202	1.6003	1.7165	1.1874	1.3418	1.2529
P_1 = 5 kN	1.9891	1.1592	1.3937	1.2279	2.3361	1.2971	0.69245	0.50940	0.03532	0.17090
P_1 = 15 kN	0.68236	0.44792	-0.202	-0.1347	1.1680	0.69063	-1.3555	-0.84660	-2.5775	-1.9930
P_1 = 25 kN	-0.6246	-0.2635	-1.798	-1.4976	-0.0003	0.08403	-3.4035	-2.2027	-5.1905	-4.1568

Table 5 Effect of plate stiffness as a function of the variation of the prestressing force of interfacial shear and normal stresses - Strengthened in Support -

Continuous RC Beam bonded with a prestressed thin plate subjected to a uniformly distributed load - *Strengthened in Support* -										
Present Model	Strengthened with Sika carbodur plate		Strengthened with four layers of Sika Wrap		Strengthened with Steel plate		Strengthened with perfect FGM plate		Strengthened with honeycomb sandwich plate	
	$\tau(x)$	$\sigma(x)$	$\tau(x)$	$\sigma(x)$	$\tau(x)$	$\sigma(x)$	$\tau(x)$	$\sigma(x)$	$\tau(x)$	$\sigma(x)$
$P_2 = 0$	0.49078	0.34785	0.40338	0.4326	0.5454	0.369472	0.31289	0.26792	0.242897	0.285403
$P_2 = 2$ kN	0.21339	0.16192	0.06454	0.0770	0.2974	0.210967	-0.12182	-0.08695	-0.31172	-0.286637
$P_2 = 5$ kN	-0.2027	-0.1169	-0.4437	-0.4536	-0.074	-0.02678	-0.77389	-0.61929	-1.14367	-1.14471
Continuous RC Beam bonded with a prestressed thin plate subjected to a Single Point Distributed Load - *Strengthened in Support* -										
Present Model	Strengthened with Sika carbodur plate		Strengthened with four layers of Sika Wrap		Strengthened with Steel plate		Strengthened with perfect FGM plate		Strengthened with honeycomb sandwich plate	
	$\tau(x)$	$\sigma(x)$	$\tau(x)$	$\sigma(x)$	$\tau(x)$	$\sigma(x)$	$\tau(x)$	$\sigma(x)$	$\tau(x)$	$\sigma(x)$
$P_2 = 0$	1.2244	0.7016	1.02553	0.8921	2.5993	1.31872	1.60624	1.01808	1.27727	0.975243
$P_2 = 2$ kN	0.9630	0.5593	0.70327	0.6195	2.1160	1.08163	0.75908	0.49504	0.196442	0.210736
$P_2 = 5$ kN	0.5510	0.3459	0.22739	0.2106	1.3911	0.7260	-0.51165	-0.28950	-1.42480	-0.936023

3.4 Effect of variation of the prestressing force of composite plate

In this section, numerical results of the present solution are presented to study the effect of the prestressing force P0 on the distribution of interfacial stress in continuous RC Beam bonded with a prestressed FRP plate. Three values of P_0 are considered in this study (P_{01} = 0 – 5 kN – 10 kN – 15 kN – 20 kN and 25 kN) and (P_{02} = 0 – 1 kN – 2 kN – 3 kN – 4 kN and 5 kN). Figs. 6 and 7 plot the interfacial shear and normal stress for the continuous RC strengthened with bonded prestressed FRP plate for the mid-point load case, from these results, one can observe:

- Maximum stress occurs at the ends of adhesively bonded plates, and the normal, or peeling, stress disappears at around 20 mm from the end of the plates.
- It is seen that increasing the value of prestressing force P_0 (P_{01} and P_{02}) leads to high stress concentrations.

The influence of the length of the ordinary-beam region (the region between the support and the end of the composite strip on the edge stresses) appears in Tables 6 and 7. It is seen that, as the plate terminates further away from the supports, the interfacial stresses increase significantly. This result reveals that in any case of strengthening, including cases where retrofitting is required in a limited zone of maximum bending moments at midspan, it is recommended to extend the strengthening strip as possible to the lines.

3.6 Effect of fiber orientation

The use of an FRP plate with different fiber orientations results changes the effective modulus

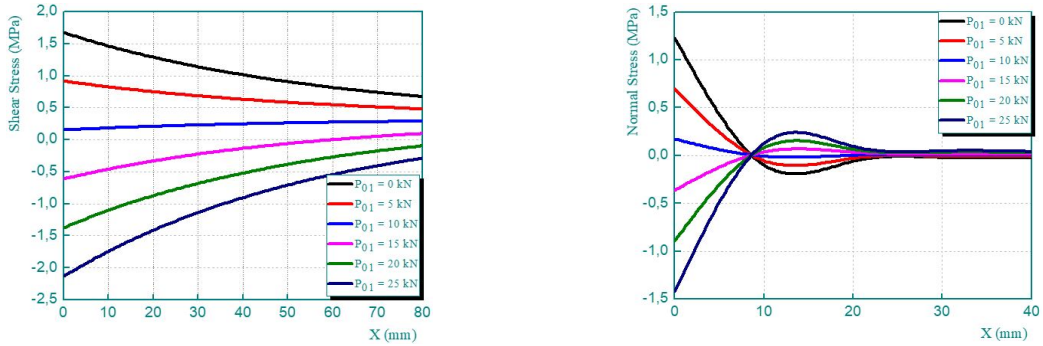

Fig. 6 Effect of the prestressing force of composite plate on interfacial stresses for a continuous RC beam strengthened with presstresed CFRP plate - ***Strengthened in Span*** -

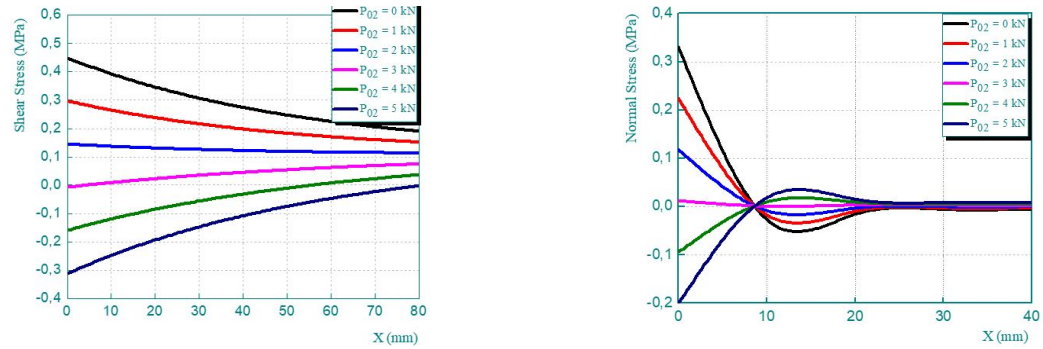

Fig. 7 Effect of the prestressing force of composite plate on interfacial stresses for a continuous RC beam strengthened with presstresed CFRP plate - ***Strengthened in Support*** -

Table 6 Effect of length of unstrengthened region "a_1" as a function of the variation of the prestressing force on the adhesion stresses

Continuous RC Beam bonded with a prestressed thin plate subjected to a uniformly distributed load - *Strengthened in Span* -					
Present model		Strengthened with Sika carbodur plate		Strengthened with four layers of Sika Wrap	
		$\tau(x)$	$\sigma(x)$	$\tau(x)$	$\sigma(x)$
a_1 = 00 mm	$P_1 = 0$	0.410424	0.236990	0.309845	0.275794
	P_1 = 25 kN	-1.12533	-0.595724	-1.59657	-1.34859
a_1 = 100 mm	$P_1 = 0$	1.03564	0.594515	0.854808	0.747475
	P_1 = 25 kN	-0.500111	-0.238199	-1.05161	-0.876905
a_1 = 200 mm	$P_1 = 0$	1.61577	0.926246	1.36070	1.18531
	P_1 = 25 kN	0.0800178	0.093532	-0.545710	-0.439074
a_1 = 300 mm	$P_1 = 0$	2.15082	1.23218	1.82755	1.58930
	P_1 = 25 kN	0.615067	0.399468	-0.0788694	-0.03508

Table 6 Continued

Continuous RC Beam bonded with a prestressed thin plate subjected to a Single Point Distributed Load - *Strengthened in Span* -					
a_1 = 00 mm	P_1 = 0	0.49126	0.65751	0.35736	0.73898
	P_1 = 25 kN	-2.7701	-3.4708	-3.6282	-7.1721
a_1 = 100 mm	P_1 = 0	1.2094	1.5867	0.96984	1.9631
	P_1 = 25 kN	-2.0520	-2.5416	-3.0157	-5.9480
a_1 = 200 mm	P_1 = 0	1.9275	2.5159	1.5824	3.1872
	P_1 = 25 kN	-1.3339	-1.6124	-2.4032	-4.7239
a_1 = 300 mm	P_1 = 0	2.6456	3.4450	2.1948	4.4113
	P_1 = 25 kN	-0.6158	-0.6833	-1.7908	-3.4998

Table 7 Effect of length of unstrengthened region "a_2" as a function of the variation of the prestressing force on the adhesion stresses

Continuous RC Beam bonded with a prestressed thin plate subjected to a uniformly distributed - *Strengthened in Support* -					
Present Model		Strengthened with Sika carbodur plate		Strengthened with four layers of Sika Wrap	
		$\tau(x)$	$\sigma(x)$	$\tau(x)$	$\sigma(x)$
a_2 = 00 mm	P_2 = 0	0.0121381	0.00852115	0.0075203	0.008172
	P_2 = 5 kN	-0.681347	-0.456295	-0.839567	-0.880726
a_2 = 200 mm	P_2 = 0	0.11979	0.0792248	0.0877603	0.094472
	P_2 = 5 kN	-0.581507	-0.385591	-0.759327	-0.764427
a_2 = 400 mm	P_2 = 0	0.333976	0.236634	0.272139	0.292068
	P_2 = 5 kN	-0.359509	-0.228182	-0.574948	-0.596831
a_2 = 600 mm	P_2 = 0	0.678131	0.480748	0.560655	0.600659
	P_2 = 5 kN	-0.015354	0.015932	-0.286432	-0.287940
Continuous RC Beam bonded with a prestressed thin plate subjected to a Single Point Distributed Load - *Strengthened in Support* -					
a_2 = 00 mm	P_2 = 0	0.145357	0.0838987	0.105640	0.0940242
	P_2 = 5 kN	-0.508050	-0.271794	-0.692496	-0.587405
a_2 = 200 mm	P_2 = 0	0.576973	0.330975	0.473594	0.413234
	P_2 = 5 kN	-0.076434	-0.024718	-0.324542	-0.268195
a_2 = 400 mm	P_2 = 0	1.00859	0.578051	0.841548	0.732444
	P_2 = 5 kN	0.355182	0.222358	0.043412	0.051015
a_2 = 600 mm	P_2 = 0	1.44021	0.825127	1.20950	1.05165
	P_2 = 5 kN	0.786800	0.469434	0.411364	0.370225

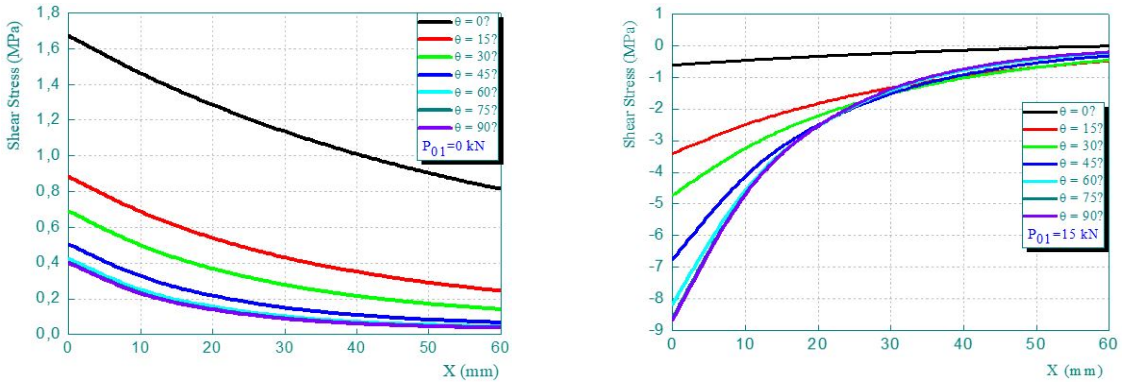

Fig. 8 Effect of fiber orientation on interfacial stresses for a continuous RC beam strengthened with presstresed CFRP plate **- *Strengthened in Span* -**

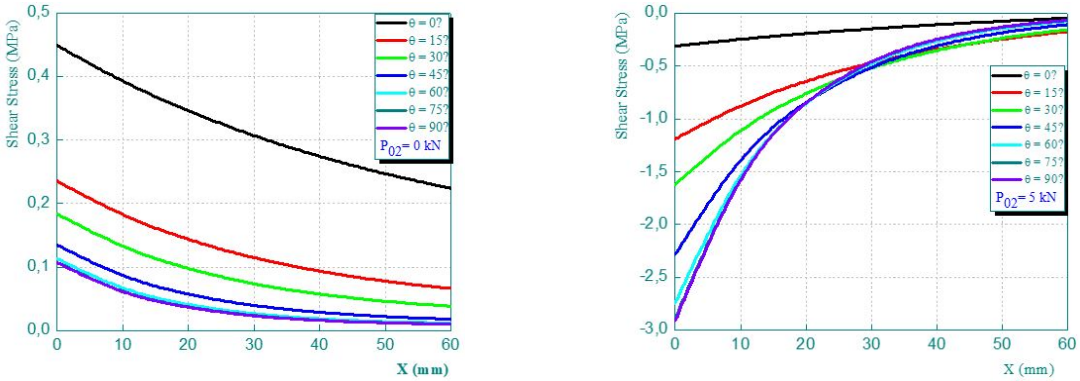

Fig. 9 Effect of fiber orientation on interfacial stresses for a continuous RC beam strengthened with presstresed CFRP plate - ***Strengthened in Support* -**

E_{eff} of the composite plate. Having high strength fibers aligned in the beam direction would maximize the modulus of the plate, while having the fibers aligned perpendicularly to the beam axis would greatly reduce the plate modulus. The effects on adhesive stresses with different fiber orientation measured from the beam's longitudinal direction are shown in Fig. 8 (Strengthened in Span) and Fig. 9 (Strengthened in Support). The maximum interfacial stress decreases with increasing alignment of all high strength fibers in the composite plate in beam's longitudinal direction x.

4. Conclusions

This paper has been concerned with the prediction of interfacial shear and normal stresses in continuous RC beam retrofitted with externally presstresed advanced composite materials. Such interfacial stresses provide the basis for understanding debonding failures in such beams and for development of suitable design rules. The adherend shear deformations have been included in the theoretical analyses by assuming linear shear stress distributions through the thickness of the

adherends. Numerical comparison between the existing solutions and the present new solution has been carried out. The present solution is general in nature and may be applicable to all kinds of materials. In the final part of this paper, extensive parametric studies were undertaken by using the new solution for strengthened beams with various ratios of design parameters. Observations were made based on the numerical results concerning their possible implications to practical designs.

Acknowledgments

This research was supported by the Algerian Ministry of Higher Education and Scientific Research (MESRS) as part of the grant for the PRFU research project n° A01L02UN140120200002 and by the University of Tiaret, in Algeria.

References

Abderezak, R., Rabia, B., Daouadji, T.H., Abbes, B., Belkacem, A. and Abbes, F. (2019), "Elastic analysis of interfacial stresses in prestressed PFGM-RC hybrid beams", *Adv. Mater. Res., Int. J.*, **7**(2), 83-103. https://doi.org/10.12989/amr.2018.7.2.083

Abderezak, R., Daouadji, T.H. and Rabia, B. (2020), "Analysis of interfacial stresses of the reinforced concrete foundation beams repairing with composite materials plate", *Coupl. Syst. Mech., Int. J.*, **9**(5), 473-498. http://doi.org/10.12989/csm.2020.9.5.473

Abderezak, R., Daouadji, T.H. and Rabia, B. (2021a), "Modeling and analysis of the imperfect FGM-damaged RC hybrid beams", *Adv. Computat. Des., Int. J.*, **6**(2), 117-133. http://doi.org/10.12989/acd.2021.6.2.117

Abderezak, R., Daouadji, T.H. and Rabia, B. (2021b), "Aluminum beam reinforced by externally bonded composite materials", *Adv. Mater. Res., Int. J.*, **10**(1), 23-44. http://doi.org/10.12989/amr.2021.10.1.023

Abderezak, R., Tahar, H.D., Rabia, B. and Tounsi, A. (2021c), "Mechanical behavior of RC cantilever beams strengthened with FRP laminate plate", *Adv. Computat. Des., Int. J.*, **6**(3), 169-190. http://doi.org/10.12989/acd.2021.6.3.169

Abderezak, R., Tahar, H.D., Rabia, B. and Tounsi, A. (2021d), "New proposal for flexural strengthening of a continuous I-steel beam using FRP laminate under thermo-mechanical loading", *Struct. Eng. Mech., Int. J.*, **78**(6), 703-714. http://doi.org/10.12989/sem.2021.78.6.703

Abderezak, R., Daouadji, T.H. and Rabia, B. (2021e), "Fiber reinforced polymer in civil engineering: Shear lag effect on damaged RC cantilever beams bonded by prestressed plate", *Coupl. Syst. Mech., Int. J.*, **10**(4), 299-316. http://doi.org/10.12989/csm.2021.10.4.299

Abderezak, R., Daouadji, T.H. and Rabia, B. (2021f), "New solution for damaged porous RC cantilever beamsstrengthening by composite plate", *Adv. Mater. Res., Int. J.*, **10**(3), 169-194. http://doi.org/10.12989/amr.2021.10.3.169

Aicha, K., Rabia, B., Daouadji, T.H. and Bouzidene, A. (2020), "Effect of porosity distribution rate for bending analysis of imperfect FGM plates resting on Winkler-Pasternak foundations under various boundary conditions", *Coupl. Syst. Mech., Int. J.*, **9**(6), 575-597. http://doi.org/10.12989/csm.2020.9.6.575

Anil, K.L., Panda, S.K., Sharma, N., Hirwani, C.K. and Topal, U. (2020), "Optimal fiber volume fraction prediction of layered composite using frequency constraints- A hybrid FEM approach", *Comput. Concrete, Int. J.*, **25**(4), 303-310. http://doi.org/10.12989/cac.2020.25.4.303

Antar, K., Amara, K., Benyoucef, S., Bouazza, M. and Ellali, M. (2019), "Hygrothermal effects on the behavior of reinforced-concrete beams strengthened by bonded composite laminate plates", *Struct. Eng. Mech., Int. J.*, **69**(3), 327-334. https://doi.org/10.12989/sem.2019.69.3.327

Benachour, A., Benyoucef, S. and Tounsi, A. (2008), "Interfacial stress analysis of steel beams reinforced with bonded prestressed FRP plate", *Eng. Struct.*, **30**, 3305-3315. https://doi.org/10.1016/j.engstruct.2008.05.007

Benferhat, R., Daouadji, T.H. and Abderezak, R. (2020a), "Thermo-mechanical behavior of porous FG plate resting on the Winkler-Pasternak foundation", *Coupl. Syst. Mech., Int. J.*, **9**(6), 499-519. http://doi.org/10.12989/csm.2020.9.6.499

Benferhat, R., Daouadji, T.H. and Abderezak, R. (2020b), "Predictions of the maximum plate end stresses of imperfect FRP strengthened RC beams: study and analysis", *Adv. Mater. Res., Int. J.*, **9**(4), 265-287. http://doi.org/10.12989/amr.2020.9.4.265

Benferhat, R., Daouadji, T.H. and Abderezak, R. (2021a), "Effect of porosity on fundamental frequencies of FGM sandwich plates", *Compos. Mater. Eng., Int. J.*, **3**(1), 25-40. http://doi.org/10.12989/cme.2021.3.1.025

Benferhat, R., Daouadji, T.H. and Abderezak, R. (2021b), "Effect of air bubbles in concrete on the mechanical behavior of RC beams strengthened in flexion by externally bonded FRP plates under uniformly distributed loading", *Compos. Mater. Eng., Int. J.*, **3**(1), 41-55. http://doi.org/ 10.12989/cme.2021.3.1.041

Benferhat, R., Daouadji, T.H. and Abderezak, R. (2021c), "Analysis and sizing of RC beams reinforced by external bonding of imperfect functionally graded plate", *Adv. Mater. Res., Int. J.*, **10**(2), 77-98. http://doi.org/10.12989/amr.2021.10.2.077

Bensattalah, T., Hassaine Daouadji, T. and Zidour, M. (2020), "Influences the Shape of the Floor on the Behavior of Buildings Under Seismic Effect", *Proceedings of the 4th International Symposium on Materials and Sustainable Development*, pp. 26-42. https://doi.org/10.1007/978-3-030-43268-3_3

Chedad, A., Daouadji, T.H., Abderezak, R., Belkacem, A., Abbes, B., Benferhat, R. and Abbes, F. (2018), "A high-order closed-form solution for interfacial stresses in externally sandwich FGM plated RC beams", *Adv. Mater. Res., Int. J.*, **6**(4), 317-328. https://doi.org/10.12989/amr.2017.6.4.317

Chen, H., Song, H., Li, Y. and Safarpour, M. (2020), "Hygro-thermal buckling analysis of polymer–CNT–fiber-laminated nano-composite disk under uniform lateral pressure with the aid of GDQM", *Eng. Comput.* https://doi.org/10.1007/s00366-020-01102-y

Cheng, X., Zhang, J., Cheng, Y., Guo, X. and Huang, W. (2020), "Effect of curing condition on mechanical properties of scarf-repaired composite laminates", *Steel Compos. Struct., Int. J.*, **37**(4), 419-429. https://doi.org/10.12989/scs.2020.37.4.419

Civalek, Ö. and Avcar, M. (2020a), "Free vibration and buckling analyses of CNT reinforced laminated non-rectangular plates by discrete singular convolution method", *Eng. Comput.* https://doi.org/10.1007/s00366-020-01168-8

Civalek, Ö. and Avcar, M. (2020b), "Free vibration and buckling analyses of CNT reinforced laminated non-rectangular plates by discrete singular convolution method", *Eng. Comput.* https://doi.org/10.1007/s00366-020-01168-8

Daraei, B., Shojaee, S. and Hamzehei-Javaran, S. (2020), "Free vibration analysis of axially moving laminated beams with axial tension based on 1D refined theories using Carrera unified formulation", *Steel Compos. Struct., Int. J.*, **37**(1), 37-49. https://doi.org/10.12989/scs.2020.37.1.037

Daouadji, T.H. (2017), "Analytical and numerical modeling of interfacial stresses in beams bonded with a thin plate", *Adv. Computat. Des., Int. J.*, **2**(1), 57-69. https://doi.org/10.12989/acd.2017.2.1.057

Daouadji, T.H., Boussad, A., Abderezak, R., Benferhat, R., Fazilay, A. and Belkacem, A. (2019), "Flexural behaviour of steel beams reinforced by carbon fibre reinforced polymer: Experimental and numerical study", *Struct. Eng. Mech., Int. J.*, **72**(4), 409-419. https://doi.org/10.12989/sem.2019.72.4.409

Daouadji, T.H., Abderezak, R. and Benferhat, R. (2020), "Flexural performance of wooden beams strengthened by composite plate", *Struct. Monitor. Maint., Int. J.*, **7**(3), 233-259. http://doi.org/10.12989/smm.2020.7.3.233

Daouadji, T.H., Tayeb, B., Abderezak, R. and Tounsi, A. (2021a), "New approach of composite wooden beam-reinforced concrete slab strengthened by external bonding of prestressed composite plate: Analysis and modeling", *Struct. Eng. Mech., Int. J.*, **78**(3), 319-332. http://doi.org/10.12989/sem.2021.78.3.319

Daouadji, T.H., Abderezak, R., Benferhat, R. and Tounsi, A. (2021b), "Performance of damaged RC continuous beams strengthened by prestressed laminates plate: Impact of mechanical and thermal properties on interfacial stresses", *Coupl. Syst. Mech., Int. J.*, **10**(2), 161-184. http://doi.org/10.12989/csm.2021.10.2.161

Daouadji, T.H., Abderezak, R., Benferhat, R. and Tounsi, A. (2021c), "Impact of thermal effects in FRP-RC hybrid cantilever beams", *Struct. Eng. Mech., Int. J.*, **78**(5), 573-583. http://doi.org/10.12989/sem.2021.78.5.573

Daouadji, T.H., Abderezak, R. and Benferhat, R. (2021d), "A new model for adhesive shear stress in damaged RC cantilever beam strengthened by composite plate taking into account the effect of creep and shrinkage", *Struct. Eng. Mech., Int. J.*, **79**(5), 531-540. http://doi.org/10.12989/sem.2021.79.5.531

Daouadji, T.H., Abderezak, R. and Benferhat, R. (2021e), "Hyperstatic steel structure strengthened with prestressed carbon/glass hybrid laminated plate", *Coupl. Syst. Mech., Int. J.*, **10**(5), 393-414. https://doi.org/10.12989/csm.2021.10.5.393

Gomes, G.F., de Almeida, F.A., Ancelotti, A.C. and da Cunha, S.S. (2021), "Inverse structural damage identification problem in CFRP laminated plates using SFO algorithm based on strain fields", *Eng. Comput.*, **37**, 3771-3791. https://doi.org/10.1007/s00366-020-01027-6

Guenaneche, B. and Tounsi, A. (2014), "Effect of shear deformation on interfacial stress analysis in plated beams under arbitrary loading", *Adhes. Adhes.*, **48**, 1-13. https://doi.org/10.1016/j.ijadhadh.2013.09.016

Hadj, B., Benferhat, R. and Daouadji, T.H. (2021), "Vibration analysis of porous FGM plate resting on elastic foundations: Effect of the distribution shape of porosity", *Coupl. Syst. Mech., Int. J.*, **10**(1), 61-77. http://doi.org/10.12989/csm.2021.10.1.061

He, X.J., Zhou, C.Y. and Wang, Y. (2019), "Interfacial stresses in reinforced concrete cantilever members strengthened with fibre-reinforced polymer laminates", *Adv. Struct. Eng.*, **23**(2), 277-288. https://doi.org/10.1177/1369433219868933

Henni, M.A.B., Abbes, B., Daouadji, T.H., Abbes, F. and Adim, B. (2021), "Numerical modeling of hygrothermal effect on the dynamic behavior of hybrid composite plates", *Steel Compos. Struct., Int. J.*, **39**(6), 751-763. http://doi.org/10.12989/scs.2021.39.6.751

Henriques, D., Goncalves, R., Sousa, C. and Camotim, D. (2020), "GBT-based time-dependent analysis of steel-concrete composite beams including shear lag and concrete cracking effects", *Thin-Wall. Struct.*, **150**, 106706. https://doi.org/10.1016/j.tws.2020.106706

Hirwani, C.K. and Panda, S.K. (2020), "Nonlinear transient analysis of delaminated curved composite structure under blast/pulse load", *Eng. Comput.*, **36**, 1201-1214. https://doi.org/10.1007/s00366-019-00757-6

Kalita, K., Dey, P., Haldar, S. and Gao, X.Z. (2020), "Optimizing frequencies of skew composite laminates with metaheuristic algorithms", *Eng. Comput.*, **36**, 741-761. https://doi.org/10.1007/s00366-019-00728-x

Keshav, V. and Patel, S.N. (2020), "Non-Linear dynamic pulse buckling of laminated composite curved panels", *Struct. Eng. Mech., Int. J.*, **73**(2), 181-190. http://doi.org/10.12989/sem.2020.73.2.181

Krour, B., Bernard, F. and Tounsi, A. (2014), "Fibers orientation optimization for concrete beam strengthened with a CFRP bonded plate: A coupled analytical-numerical investigation", *Eng. Struct.*, **56**, 218-227. https://doi.org/10.1016/j.engstruct.2013.05.008

Larrinaga, P., Garmendia, L., Piñero, I. and San-José, J.T. (2020), "Flexural strengthening of low-grade reinforced concrete beams with compatible composite material: Steel Reinforced Grout (SRG)", *Constr. Build. Mater.*, **235**, 117790. https://doi.org/10.1016/j.conbuildmat.2019.117790

Liu, S., Zhou, Y., Zheng, Q., Zhou, J., Jin, F. and Fan, H. (2019), "Blast responses of concrete beams reinforced with steel-GFRP composite bars", *Structures*, **22**, 200-212. https://doi.org/10.1016/j.istruc.2019.08.010

Mercan, K., Ebrahimi, F. and Civale, Ö. (2020), "Vibration of angle-ply laminated composite circular and annular plates", *Steel Compos. Struct., Int. J.*, **34**(1), 141-154. http://doi.org/10.12989/scs.2020.34.1.141

Panjehpour, M., Ali, A.A.A., Voo, Y.L. and Aznieta, F.N. (2014), "Effective compressive strength of strut in CFRP-strengthened reinforced concrete deep beams following ACI 318-11", *Comput. Concrete, Int. J.*,

13(1), 135-165. https://doi.org/10.12989/cac.2014.13.1.135
Panjehpour, M., Farzadnia, N., Demirboga, R. and Ali, A.A.A. (2016), "Behavior of high-strength concrete cylinders repaired with CFRP sheets", *J. Civil Eng. Manag.*, **22**(1), 56-64. https://doi.org/10.3846/13923730.2014.897965
Rabahi, A., Daouadji, T.H., Abbes, B. and Adim, B. (2016), "Analytical and numerical solution of the interfacial stress in reinforced-concrete beams reinforced with bonded prestressed composite plate", *J. Reinf. Plast. Compos.*, **35**(3), 258-272. https://doi.org/10.1177/0731684415613633
Shahmohammadi, M.A., Azhari, M. and Saadatpour, M.M. (2020), "Free vibration analysis of sandwich FGM shells using isogeometric B-spline finite strip method", *Steel Compos. Struct., Int. J.*, **34**(3), 361-376. https://doi.org/10.12989/scs.2020.34.3.361
Smith, S.T. and Teng, J.G. (2002), "Interfacial stresses in plated beams", *Eng. Struct.*, **23**(7), 857-871. http://doi.org/10.1016/S0141-0296(00)00090-0
Tanzadeh, H. and Amoushahi, H. (2020), "Analysis of laminated composite plates based on different shear deformation plate theories", *Struct. Eng. Mech., Int. J.*, **75**(2), 247-269. http://doi.org/10.12989/sem.2020.75.2.247
Tayeb, B., Daouadji, T.H., Abderezak, R. and Tounsi, A. (2021), "Structural bonding for civil engineering structures: New model of composite I-steel-concrete beam strengthened with CFRP plate", *Steel Compos. Struct., Int. J.*, **41**(3), 417-435. https://doi.org/10.12989/scs.2021.41.3.417
Tlidji, Y., Benferhat, R. and Daouadji, T.H. (2021a), "Study and analysis of the free vibration for FGM microbeam containing various distribution shape of porosity", *Struct. Eng. Mech., Int. J.*, **77**(2), 217-229. http://doi.org/10.12989/sem.2021.77.2.217
Tlidji, Y., Benferhat, R., Trinh, L.C., Daouadji, T.H. and Tounsi, A. (2021b), "New state-space approach to dynamic analysis of porous FG beam under different boundary conditions", *Adv. Nano Res., Int. J.*, **11**(4), 347-359. https://doi.org/10.12989/.2021.11.4.347
Tounsi, A. (2006), "Improved theoretical solution for interfacial stresses in concrete beams strengthened with FRP plate", *Int. J. Solids Struct.*, **43**(14-15), 4154-4174. https://doi.org/10.1016/j.ijsolstr.2005.03.074
Tounsi, A., Daouadji, T.H. and Benyoucef, S. (2008), "Interfacial stresses in FRP-plated RC beams: Effect of adherend shear deformations", *Int. J. Adhes. Adhes.*, **29**, 313-351. https://doi.org/10.1016/j.ijadhadh.2008.06.008
Wang, L., Yang, J. and Li, Y.H. (2021), "Nonlinear vibration of a deploying laminated Rayleigh beam with a spinning motion in hygrothermal environment", *Eng. Comput.*, **37**, 3825-3841. https://doi.org/10.1007/s00366-020-01035-6
Wang, H., Yan, W. and Li, C. (2020a), "Response of angle-ply laminated cylindrical shells with surface-bonded piezoelectric layers", *Struct. Eng. Mech., Int. J.*, **76**(5), 599-611. http://doi.org/10.12989/sem.2020.76.5.599
Wang, Y.H., Yu, J., Liu, J.P., Zhou, B.X. and Chen, Y.F. (2020b), "Experimental study on assembled monolithic steel-prestressed concrete composite beam in negative moment", *J. Constr. Steel Res.*, **167**, 105667. https://doi.org/10.1016/j.jcsr.2019.06.004
Yuan, C., Chen, W., Pham, T.M. and Hao, H. (2019), "Effect of aggregate size on bond behaviour between basalt fibre reinforced polymer sheets and concrete", *Compos. Part B: Eng.*, **158**, 459-474. https://doi.org/10.1016/j.compositesb.2018.09.089
Zeverdejani, M.K. and Beni, Y.T. (2020), "Effect of laminate configuration on the free vibration/buckling of FG Graphene composites", *Adv. Nano Res., Int. J.*, **8**(2), 103-114. http://doi.org/10.12989/anr.2020.8.2.103
Zohra, A., Benferhat, R., Tahar, H.D. and Tounsi, A. (2021), "Analysis on the buckling of imperfect functionally graded sandwich plates using new modified power-law formulations", *Struct. Eng. Mech., Int. J.*, **77**(6), 797-807. http://doi.org/10.12989/sem.2021.77.6.797

CC